*Remote Sens.* **2014**, *6*, 11673-11688; doi:10.3390/rs61211673

OPEN ACCESS

*remote sensing*

**ISSN 2072-4292**

www.mdpi.com/journal/remotesensing

*Article*

# Separating Mangrove Species and Conditions Using Laboratory Hyperspectral Data: A Case Study of a Degraded Mangrove Forest of the Mexican Pacific

**Chunhua Zhang [1,*], John M. Kovacs [2], Yali Liu [3], Francisco Flores-Verdugo [4] and Francisco Flores-de-Santiago [5]**

1 Department of Geography and Geology, Algoma University, 1520 Queen Street East, Sault Ste. Marie, ON P6A 2G4, Canada

2 Department of Geography, Nipissing University, 100 College Drive, North Bay, ON P1B 8L7, Canada; E-Mail: johnmk@nipissingu.ca

3 Department of Mathematics and Statistics, East Tennessee State University, Johnson City, TN 37614, USA; E-Mail: LIUY01@mail.etsu.edu

4 Instituto del Ciencias del Mar y Limnología, Universidad Nacional Autónoma de México, Mazatlán, SIN 82040, México; E-Mail: ffverdugo@gmail.com

5 Instituto de Ciencias del Mar y Limnología, Universidad Nacional Autónoma de México, A.P. 70-305, Av. Universidad 3000, Ciudad Universitaria, Coyoacán D.F. 04510, México; E-Mail: ffloresd@cmarl.unam.mx

* Author to whom correspondence should be addressed; E-Mail: chunhua.zhang@algomau.ca; Tel.: +1-705-949-2301; Fax: +1-705-949-6583.

External Editors: Randolph H. Wynne and Prasad S. Thenkabail

*Received: 19 August 2014; in revised form: 18 November 2014 / Accepted: 19 November 2014 / Published: 25 November 2014*

---

**Abstract:** Given the scale and rate of mangrove loss globally, it is increasingly important to map and monitor mangrove forest health in a timely fashion. This study aims to identify the conditions of mangroves in a coastal lagoon south of the city of Mazatlán, Mexico, using proximal hyperspectral remote sensing techniques. The dominant mangrove species in this area includes the red (*Rhizophora mangle*), the black (*Avicennia germinans*) and the white (*Laguncularia racemosa*) mangrove. Moreover, large patches of poor condition black and red mangrove and healthy dwarf black mangrove are commonly found. Mangrove leaves were collected from this forest representing all of the aforementioned species and conditions. The leaves were then transported to a laboratory for spectral measurements using an ASD

FieldSpec® 3 JR spectroradiometer (Analytical Spectral Devices, Inc., USA). $R^2$ plot, principal components analysis and stepwise discriminant analyses were then used to select wavebands deemed most appropriate for further mangrove classification. Specifically, the wavebands at 520, 560, 650, 710, 760, 2100 and 2230 nm were selected, which correspond to chlorophyll absorption, red edge, starch, cellulose, nitrogen and protein regions of the spectrum. The classification and validation indicate that these wavebands are capable of identifying mangrove species and mangrove conditions common to this degraded forest with an overall accuracy and $K_{hat}$ coefficient higher than 90% and 0.9, respectively. Although lower in accuracy, the classifications of the stressed (poor condition and dwarf) mangroves were found to be satisfactory with accuracies higher than 80%. The results of this study indicate that it could be possible to apply laboratory hyperspectral data for classifying mangroves, not only at the species level, but also according to their health conditions.

**Keywords:** mangrove; degradation; hyperspectral remote sensing; classification; Mexico

## 1. Introduction

Mangrove forests represent wetlands of local, regional and even global importance. Locally, mangroves provide a variety of renewable resources and are critical to the health of fisheries. Regionally and globally, mangrove forests are considered key carbon sinks and play an important role as an indispensable habitat for a variety of aquatic and terrestrial organisms. However, mangrove forests have experienced a worldwide degradation due to several reasons, such as pollution, hydrological changes, aquaculture, recreational activities, climate changes, *etc.* Degraded mangrove forests generally have lower productivity and, thus, provide less ecosystem goods and services than their healthier counterparts. It is thus crucial that resource managers be able to map and monitor mangrove forests at increasing levels of detail, including species distribution and health condition.

Traditional field work is time consuming, costly and sometimes just simply impossible for wetland vegetation communities. As a result, remote sensing techniques have been widely applied to map mangrove distribution. The most commonly employed imagery types are based on multi-spectral bands, such as Landsat (e.g., [1–3]) and SPOT (e.g., [3–6]). However, the steep environmental gradient and the coarse image spectral and spatial resolutions can limit the effectiveness of mapping mangroves [7]. As a consequence, hyperspectral remote sensing techniques, where very large numbers of bands are available (*i.e.*, typically greater than 20), have been shown to be a potential alternative source of data for monitoring wetland vegetation [7], including mangroves [8–10]. Spectral responses could be different for various hyperspectral wavebands. In fact, chemical absorption regions have been used to separate vegetation species, due to differences in leaf color, leaf cell structure and leaf chemical components. To date, there have been several examples of applications of hyperspectral images on mangrove forests. Airborne hyperspectral instruments, such as Airborne Visible/Infrared Imaging Spectrometer (AVIRIS) (e.g., [11]), Compact Airborne Spectrographic Imager (CASI) [12–14] and Airborne Imaging Spectrometer for Application (AISA+) [15], and satellite hyperspectral imagery (Hyperion) (e.g., [16,17]) have been used for monitoring and classifying mangrove species. The results from these studies would

suggest that classifications based on hyperspectral imagery can provide satisfactory results for mapping mangrove communities. However, mangrove forests are experiencing rapid rates of degradation due to climate change and other more obvious anthropogenic disturbances, such as hydrological modifications, aquaculture expansion and pollutants [18]. Unfortunately, there have not been any studies that apply hyperspectral data for classifying mangrove health in degraded areas. Moreover, prior to any application of hyperspectral satellite imagery in mapping mangroves, it is necessary to test the feasibility of applying laboratory-based hyperspectral data for identifying mangrove species under various health conditions.

It is challenging to separate vegetation species using spectral measurement due to spectral similarity amongst species. In addition, the large number of wavebands available (*i.e.*, high dimensionality) imposes the problem of high computational cost, the so-called "Hughes phenomenon" or "the curse of dimensionality" [19–22]. Furthermore, there are typically strong correlations between closely neighboring spectral wavebands. The correlation (*i.e*., redundant information) might indicate a high risk of over fitting for classification [23,24]. Consequently, it is critical to select the most useful wavebands from hyperspectral data for accurate species/condition separation.

Currently, there are many studies published regarding the separation of vegetation species using hyperspectral data (e.g., [25,26]). However, only a few studies have applied laboratory hyperspectral data to separate mangrove species. Vaiphasa *et al.* [27] identified sixteen mangrove species in Thailand using analysis of variance (ANOVA) and Jeffries-Matusita distance. Kamaruzaman and Kasawani [28] separated five mangrove species by applying stepwise discriminant analysis. Similarly, Mochel and Ponzoni identified the separability of four mangrove species located in northern Brazil [29]. Wang and Sousa [30] separated three mangrove species with laboratory hyperspectral reflectance using linear discriminant analysis. Mochel and Ponzoni [29] and Wang and Sousa [30] also applied ANOVA to test the spectral differences of mangroves. None of these previous studies examined the separability of mangrove species with various conditions using laboratory hyperspectral data. While ANOVA could be used to identify the significance of differences, previous studies [30] did not show the efficacies (error matrices and $K_{hat}$ coefficient) of applying hyperspectral data for identifying species condition. This is probably because of the challenge in dealing with similarity in their spectral response. Therefore, our objective was to examine the feasibility of separating three mangrove species with several health conditions using laboratory hyperspectral reflectance data, which could result in identifying the most optimal bands for these endeavors.

## 2. Study Area

The mangrove forest is located in a coastal lagoon south of the city of Mazatlán in the Mexican State of Sinaloa (23°19′N, 106°19′W). This region is characterized by a sub-tropical, semi-arid climate with a distinct dry and rain season. It is important to mention that the black mangrove (*Avicennia germinans*) dominates this area, and based on height, leaf color and distance to the water's edge, this black mangrove could be classified according to three conditions: Healthy, dwarf healthy and poor condition (Figure 1a,b,c). Healthy mangroves are generally located close to the main tidal channel, with an average height between 4 and 5 m. The healthy black mangroves (Figure 1a) are found mixed with red mangroves (*Rhizophora mangle*) and some white mangroves (*Laguncularia racemosa*) within a very thin fringe along the main tidal channel. The dwarf black mangroves (Figure 1b) and the poor condition black mangroves

(Figure 1c) are found more inland, where the tidal influence is low [31]. Their height is generally around 1 to 1.5 m, and their leaves are smaller and thicker than for those of healthy ones. Dwarf mangrove forests are found in sub-optimal conditions (e.g., P-limited). The healthy red (Figure 1d) and white (Figure 1e) mangroves are generally found along the water's edge, where daily semi-diurnal tidal flushing is the norm. Stressed red mangroves are located more inland near the transition zone from the healthy black to the dwarf and poor condition black mangroves (Figure 1f).Their leaves typically have a yellowish coloration, and the tree canopy is much sparser compared with their healthy counterparts. Numerous dead twigs and branches are present in the poor condition mangrove stands. This condition is caused by increased stress in the environment, resulting from a variety of possible causes, such as soil hypersalinity, hydrological changes or exposure to pollutants.

**Figure 1.** Mangrove forest represented by various species and different conditions. (**a**) healthy black mangrove, (**b**) dwarf black mangrove, (**c**) poor condition black mangrove, (**d**) healthy red mangrove, (**e**) healthy white mangrove and (**f**) poor condition red mangrove.

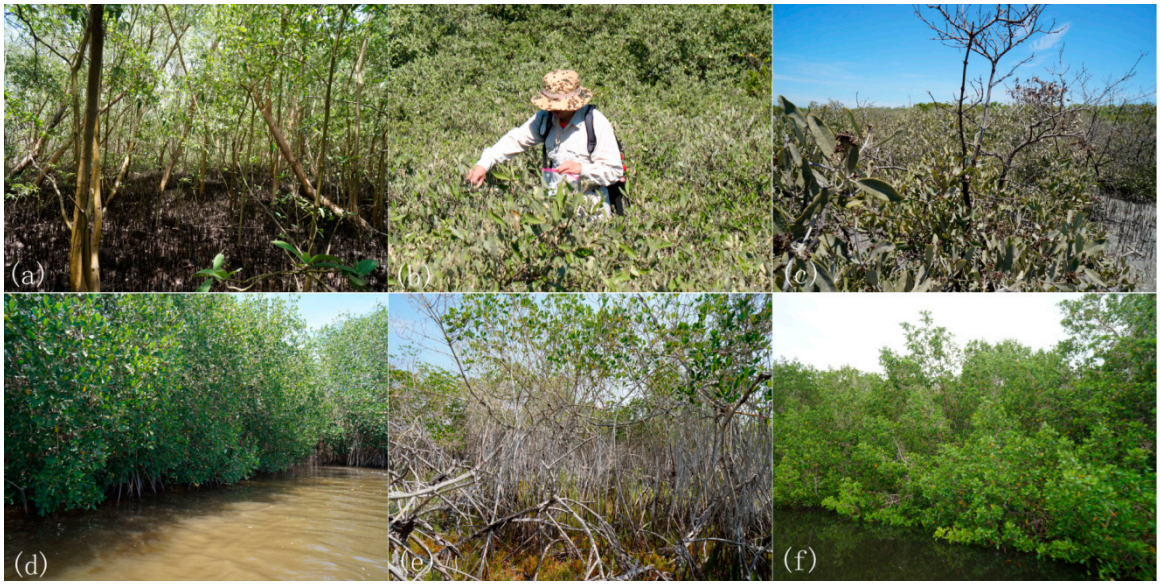


## 3. Methods

### *3.1. Field Data Collection*

Field work was conducted in mid-December, 2008 during the dry season. Leaves from the red, black and white mangroves with various conditions were collected from branches of the top canopy. Leaves were collected along the main tidal channel on a boat using an extendable hook for the healthy black, red and white mangroves. Only the third to fifth leaves from the tip were clipped from each branch, so that only mature leaves were collected. In total, 91 leaf samples of black mangrove, 60 samples of red mangrove and 30 samples of white mangrove were collected. All of the leaves were placed in plastic bags and then stored in a cooler at 4 °C for transport to the laboratory, where the reflectance data were recorded.

### *3.2. Spectral Response Measurements and Preprocessing*

An indoor black house laboratory was set up to measure the leaf spectral responses at the Instituto de Ciencias del Mar y Limnología. Leaf reflectance was measured using an ASD FieldSpec® 3 JR spectroradiometer (Analytical Spectral Devices, Inc., USA) on the same day as the leaf collection. The collection site was only three hours' travelling distance from the lab. The measurement range for this device is 350–2500 nm, and the spectral resolution 3 nm from 350 to 1000 nm and 30 nm from 1001 to 2500 nm. A 50-W halogen light was used as the light source for the indoor measurements. Two layers of mangrove leaves were stacked facing up on a matt black plate with a diameter of 25 cm. A 25° field of view sensor was mounted right above the plate at a distance of 30 cm. A white reference (Spectralon) was used to calibrate the measurements every 5 min. For each measurement, the value recorded was based on an average of 15 spectral readings. Four measurements were obtained for each sample by rotating the plate roughly 90° to avoid potential impacts from the bidirectional reflectance distribution function [27]. The final spectral reflectance number for each sample was calculated as the average of the four measurements.

To decrease the number of wavebands from the original 2150 wavebands, the data were further aggregated into 215 bands at a bandwidth of 10 nm, as neighboring wavebands provide similar (redundant) information. The name for these new aggregated wavebands was determined by the starting wavelength. For example, B420 indicates the wavelength region of 420–429 nm. Wavebands from 350 to 400 nm were not used, since they represent the ultraviolet region of the spectrum.

### *3.3. Statistical Methods*

#### 3.3.1. Waveband Selection

The squared correlation coefficient ($R^2$ plot) among all wavebands, principal components analysis (PCA) and stepwise discriminant analysis (SDA) were examined in order to identify the most ideal wavebands for the mangrove hyperspectral classification [26,32].

It is important to mention that although the wavebands were averaged prior to the statistical analyses, there were still cases of strong correlations among the averaged wavebands within the dataset, resulting in redundancy. As a consequence, the $R^2$ plot was used to select these wavebands with low correlation, thus providing complimentary information (Figure 4). Using 0.0001 as a cutoff point of correlation, a total of 77 of the least correlated waveband pairs were selected for further data classification.

The PCA is an important statistical tool, because it can efficiently reduce the large amount of wavebands from the laboratory measurements using an orthogonal transformation [8]. Following the latent root criterion, five principal components were selected, since their eigenvalues were found to be greater than 1 [33]. As a result, the five components explained 98.8% of the total observed variation. For further selection, a total of 100 wavebands, 20 wavebands from each principle, were selected based on their factor loadings.

The SDA technique can be used to select a subset of the wavebands that contributed most to the discriminatory power of the model [26]. It has commonly been used to classify spectral responses into different classes. At each step, all wavebands are evaluated within the model. Those wavebands that fail to meet the criterion to stay within the model are removed, whereas wavebands that can contribute most

to the discriminant function are retained within the model. The procedure stops when no further wavebands are removed. Using this method, a total of 54 wavebands were selected using a significance level of 0.05 for entry and removal from the model.

Wavebands from different wavelength regions are strongly associated with specific elements of the leaf biophysical structure. For example, the visible light portion is often related to the leaf pigment contents/concentration, whereas the near-infrared (NIR) is more related to the leaf structure. Moreover, the shortwave infrared is closely linked to the leaf water content. Some hyperspectral bands are also known to correspond to leaf chemical absorption [34]. As a consequence, bands from these regions of the spectrum may be particularly useful for separating mangroves according to species and conditions. To make sure the selected wavebands were not solely from the visible, NIR or short wavelength infrared regions, the spectrum was split into four sections: 400–690, 700–1350, 1360–1750 and 1760–2340 nm. Moreover, to guarantee that the selected wavebands were more practical, the wavebands in the water absorption regions were excluded from further analyses.

All selected wavebands from these methods were then pooled together. Wavebands with a frequency over three were then selected for further classification using discriminant analysis. These selected wavebands would have the weakest correlation among them and, thus, be the ideal candidates to discriminate the samples [32]. One-way ANOVA was performed for the mean reflectance at the selected wavebands in order to examine the variance among the different mangrove species and conditions.

#### 3.3.2. Mangrove Condition Classification and Validation

Discriminant analysis was applied to separate mangrove species and conditions, as it has been widely used to examine the separability of multiple category data [30,35]. This technique develops a classification criterion using a measure of generalized squared distance. Each observation is classified into a group from which it has the smallest generalized squared distance. Instead of using linear discriminant functions [30], quadratic discriminant functions, also known as the classification criterion, were used to assign group membership (see [36]), because the test of homogeneity of within-covariance matrices is significant. Classification accuracy was evaluated using the error matrices generated from the discriminant models. Total accuracy and the $K_{hat}$ coefficient were calculated based on the error matrices.

Results obtained from the discriminant analysis may only be applicable to the sample used. We required a discriminant model that has been both externally and internally validated, and therefore, cross-validation was also performed to check on the propensity to inflate the accuracy if the all of the data are being used. The classification was conducted using the leave-one-out procedure, *i.e.*, each sample was classified using the discriminant function constructed by taking that sample out of the dataset. Hence, each sample was reclassified as if it were a new unknown observation. In fact, cross-validation provides a better, but more conservative, assessment of classification accuracy.

## 4. Results and Discussion

### *4.1. Spectral Properties of Mangrove Species and Conditions*

Healthy mangroves, including the black, red and white species, have lower reflectance in the red and higher reflectance in the NIR wavelength regions ($p < 0.01$) (Figure 2). The differences in reflectance in

the visible light region are indicative of the observed variation in leaf colors. The red mangrove leaves have a dark green color and consequently have the lowest reflectance in the green and red regions of the spectrum. The white mangrove leaves typically have a bright green color and consequently have the highest reflectance in the green spectrum. Among the three species, the red mangrove has considerably higher values in the NIR wavelength region. This observation could be attributed to the very thick leaves [31], relative to other species, which could cause stronger reflectance, especially in the NIR region, as observed in our study. This may also explain why the reflectance for the dwarf red is almost as high as those of the healthy black and white mangroves within the NIR region.

**Figure 2.** Spectral profiles of the healthy and stressed mangrove classes. Healthy black, healthy red, healthy white, dwarf black, dwarf black and dwarf red).

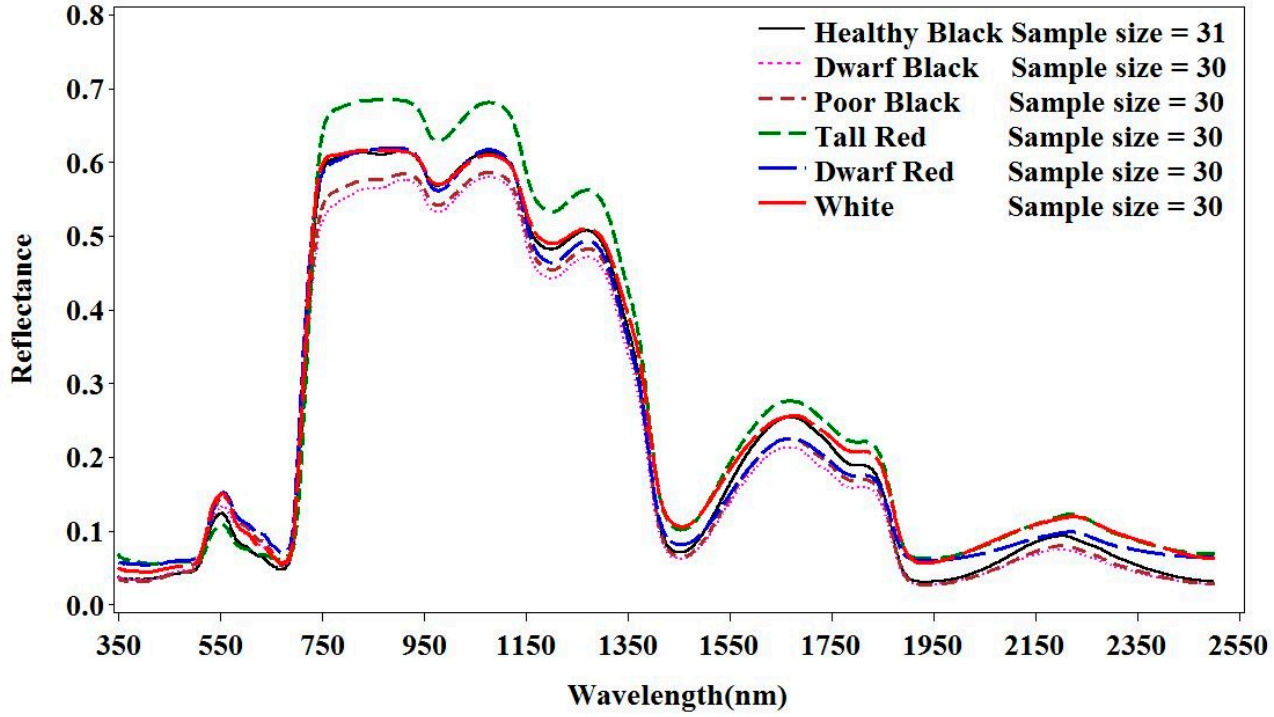


Different mangrove species and conditions exhibit various changes in their spectral responses (Figure 3). Dwarf black, poor condition black and healthy white mangroves have the lowest degree of variation, whereas dwarf red and healthy red have the highest. Among the wavelength regions, the lowest variation was found in the near-infrared region. Within-category variations in reflectance were much larger for visual light and short wavelength regions.

Stressed mangroves have stronger reflectance in visible light, particularly for the red light regions ($p < 0.01$). This is most likely the result of a drop of chlorophyll content and an increase of carotenoids in the leaves. Consequently, leaves for the stressed mangroves look yellowish. The dwarf red leaves were the most yellowish and consequently had the strongest reflectance in the red spectrum. Moreover, stressed mangrove leaves are generally smaller and thicker [31,37] and, thus, should have higher reflectance in the NIR region. In contrast, the reflectance of the stressed mangroves in our study was shown to be generally lower than the healthy mangroves in the NIR region. This could be caused by structural changes within the leaves. Consequently, the internal scattering at the cell wall-air interfaces in the leaves had decreased significantly.

**Figure 3.** Standard deviation (**top**) and coefficient of variation (**bottom**) of reflectance for each species type and conditions.

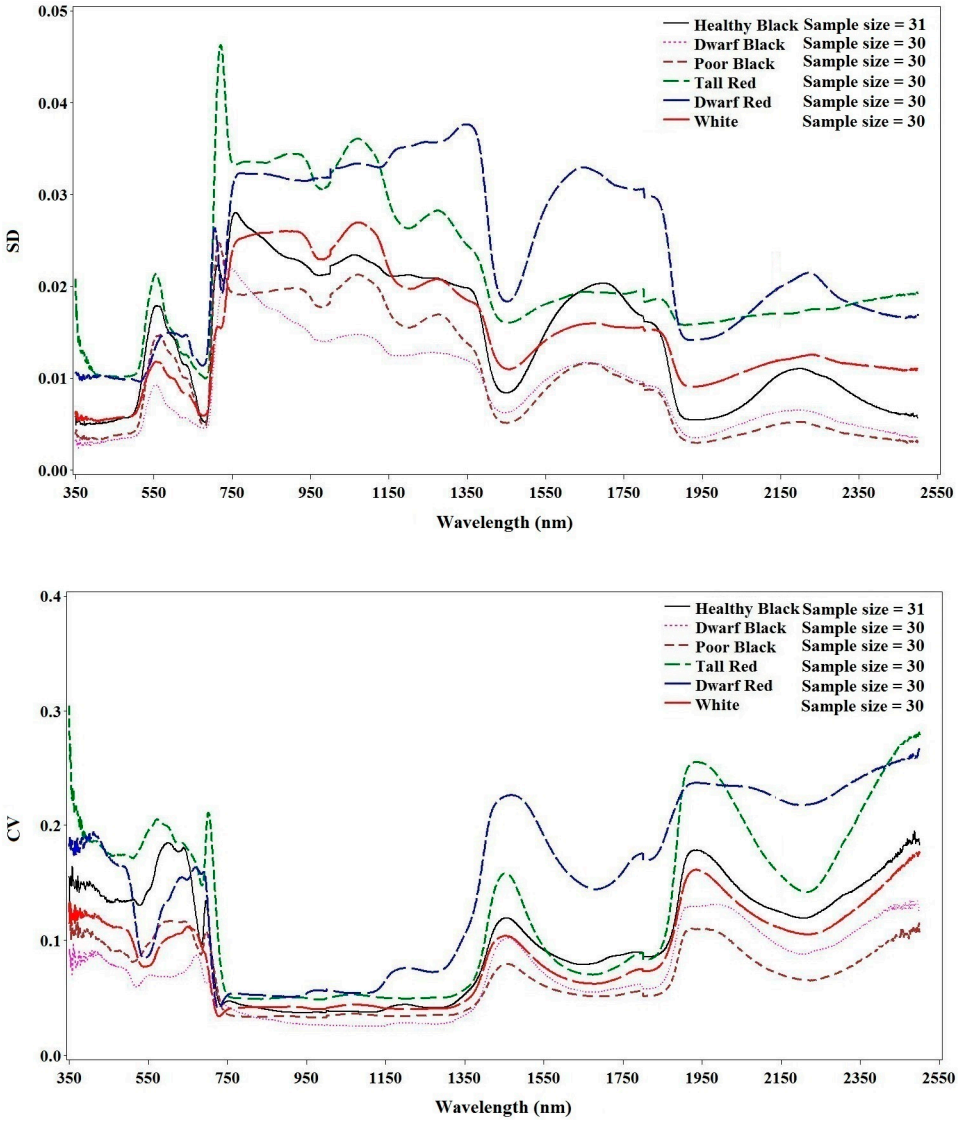


It is interesting to note that the reflectance of the dwarf black mangrove was slightly lower than that for the poor condition black mangrove even though the difference was not significant ($p > 0.01$). In contrast to healthy black mangroves, dwarf black mangroves are typically found in sub-optimal conditions generally characterized by limited nutrients and freshwater [37–40]. Consequently, their height is generally not more than 1.5 m, as observed in our study site (Figure 1). This type of sub-tropical environment might have caused significant changes in the leaf structure, resulting in the observed lower reflectance in comparison to the poor condition black mangroves in the NIR region.

It is difficult to explain why, in general, there was a higher reflectance in healthy mangroves along the short wavelength regions. Poor condition red mangroves were found to have the lowest nitrogen concentration and water content [9,10], and yet, they showed the strongest absorption in this region. Water content is one of the main determinants in the short wavelength region. This would indicate that other chemical components in the leaves, such as starch, lignin or fiber, could be associated with the observations. One other possible reason may be linked to small salt crystals that are often found on the

leaves of the poor condition and dwarf black mangroves. These salt crystals result from the tree excreting excessive minerals when dealing with hypersaline conditions typical of many stressed basin mangrove forests. When the samples were brought back to the laboratory, some of the poor condition leaf surfaces were generally wetter than the healthy leaves, due possibly to the absorption of moisture from salt crystals. This thin layer of moisture could have possibly lowered the reflectance.

### *4.2. Wavebands Selection*

As previously indicated, a frequency occurrence of greater than three was used to select bands for further classification. These bands correspond to wavelength regions of pigments absorption, red edge, nitrogen absorption, *etc.* (Table 1 and Figure 5). Only wavebands of high frequency and physiological significance were selected (Table 2). Data redundancy is a third factor of wavebands selection. Consequently, several visible light and near-infrared wavebands were not selected for further analysis. Specifically, the selected wavebands were 520 (blue-green), 560 (green), 650 (red), 710 (red edge), 760 (red edge), 2100 and 2230 nm. Six hundred fifty nanometers is the absorption region for chlorophyll b. Wavebands along the visible region and the red edge region were reported to be optimal for detecting crop nitrogen [41]. The 2100 and 2300 nm bands have been shown to correspond to the absorption regions for fiber, starch, protein and nitrogen [31].

Our results differ from other researchers in regards to the selected bands. For example, 780, 790, 800, 1480, 1530 and 1550 nm were found to be the most useful bands for separating three mangrove species [30]. This may be expected given the species we examined and, most importantly, our focus on the conditions of the mangroves, as well. Mangrove leaves of various conditions have different levels of chlorophyll content, nitrogen and water content [9,10,31]. In addition, the sensitivity of the reflectance to stress varies considerably in the visible and the NIR range [42,43]. It is important to note that no wavebands from 800–1350 nm and 1360–1750 nm were selected. The small variations in the near-infrared region (Figures 2 and 3) partly explain the reasons why no wavebands were selected for further classification analysis. Reflectance of dwarf and healthy black mangrove were almost identical from the 800 to 1350 nm wavelength region. Two red edge wavebands and three visual light wavebands were selected instead. These wavebands have been shown to be the optimal ones in identifying vegetation stress and moisture content [26]. In addition, the results from other studies also indicate that those particular wavebands might not be as useful as the wavebands selected. Results from a crop study using a similar method also indicated that visual light and the red edge wavebands are more useful in classifications [32].

**Table 1.** Wavebands selected using three statistical methods. SDA, stepwise discriminant analysis.

| Methods | Wavebands Selected (nm) | Notes |
|---|---|---|
| $R^2$ | 520–650, 690–710, 750–770, 830, 890–910, 1170, 1180, 1210–1,230, 1310–1370, 1390–1420, 1440–1490, 1510, 1520, 1550, 1560, 1630, 1640–1670, 1770, 1780, 1830, 1840, 1860, 1870, 2080–2130, 2160–2200, 2220–2240, 2280–2330 | 0.0001 is the cutoff point of correlation |

**Table 1.** *Cont.*

| Methods | Wavebands Selected (nm) | Notes |
|---|---|---|
| PCA | 450–760, 850–940, 1020–1110, 1850–1870, 1920, 1930, 1940, 2110–2270 | PC1 74.84%, PC2 14.13%, PC3 5.43%, PC4 3.15%, PC5 1.22% of variation |
| SDA | 400, 440, 450, 470, 490, 510–570, 600, 630, 650–720, 740, 1000, 1110, 1120, 1140, 1190, 1200, 1290, 1400, 1520, 1630, 1650, 1660, 1710, 1730, 1740, 1780, 1790, 1800, 1840, 1870, 1920, 1960, 2090, 2100, 2140, 2200, 2210, 2230, 2250, 2260 | Entry and stay probability is 0.05 |

**Figure 4.** $R^2$ plot. Areas of lowest $R^2$ values (<0.0001) were selected for further analysis.

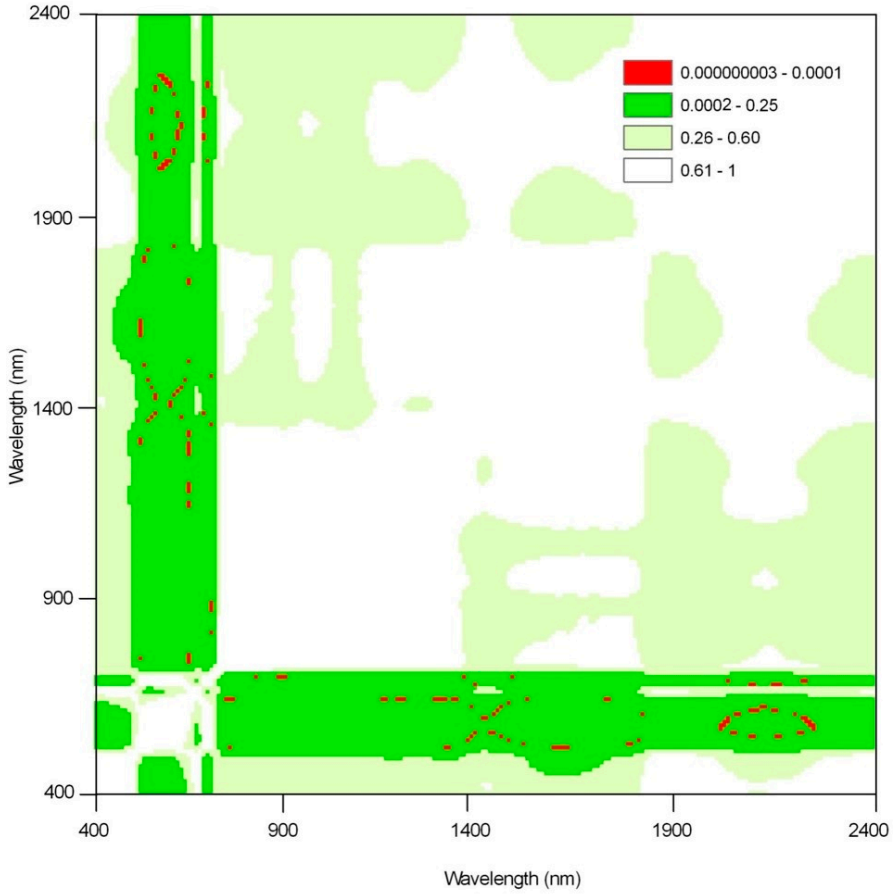


**Table 2.** Selected spectral wavebands for mangrove condition classification using three methods.

| Spectral Region (nm) | Center of Wavebands (nm) | Significance |
|---|---|---|
| 400–690 | 520, 560, 650 | Chlorophyll content |
| 700–1350 | 710, 760 | Red edge/plant stress |
| 1360–1750 | No wavebands selected | - |
| 1760–2340 | 2100, 2230 | Starch, cellulose, protein and nitrogen |

**Figure 5.** Frequency of selected wavebands using $R^2$ plot, PCA and SDA. Selected wavebands are underscored.

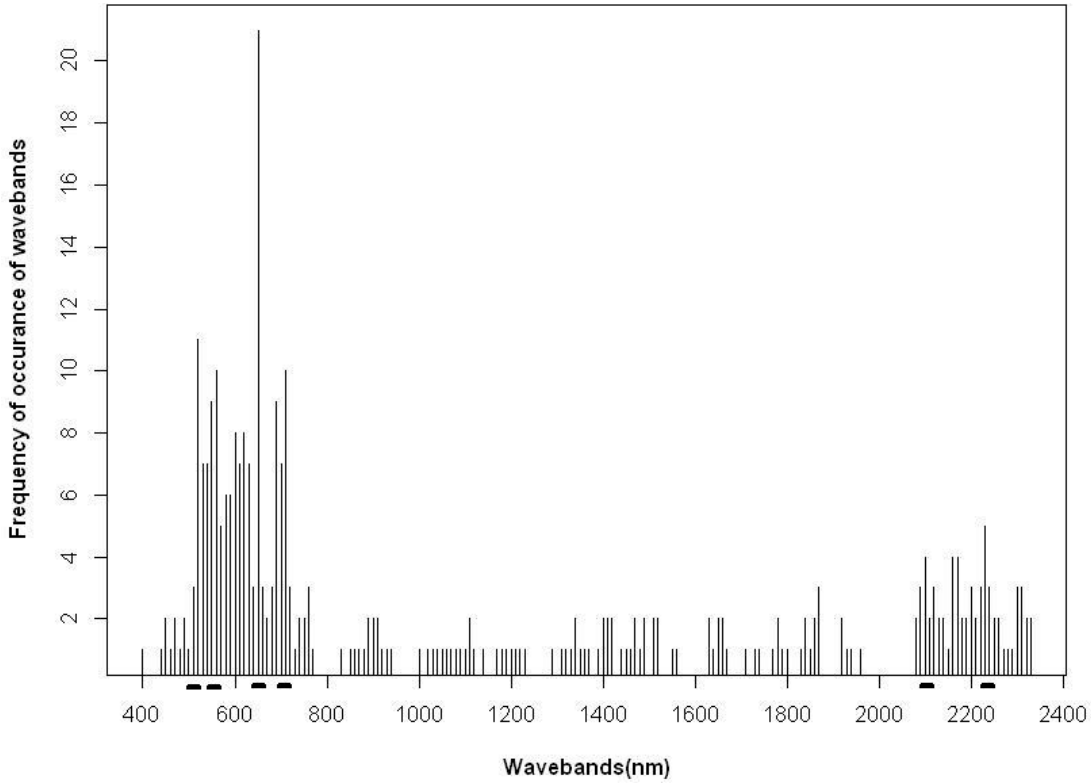


*4.3. Mangrove Classification and Validation*

The selected wavebands were found to separate the three mangrove species with different conditions quite well. Results of the classification based on these wavebands were deemed more than satisfactory (Table 3). The overall accuracy and kappa coefficient were calculated at 97.78% and 0.97, respectively. White, healthy red and dwarf red mangroves are spectrally distinct. The white mangrove had an accuracy of 100%, thus making them easy to separate from other species. The confusion is found mainly between the poor condition black, the healthy black and the dwarf black mangroves. This is obvious, since spectrally, these three conditions are similar. Nonetheless, the accuracies for dwarf and poor condition black mangroves are satisfactory, as they are all above 90%.

The validation indicates that there is only a slight drop among the accuracies (Table 4). The overall accuracy and the $K_{hat}$ were calculated at 91.7% and 0.90, respectively. Again, white and healthy red mangroves were easily separated from the other species with classification accuracies of 100%. The dwarf red mangrove is also separated with a high accuracy (96.67% for the user's accuracy and 100% for the producer's accuracy). Similarly, the confusions occur between the black mangroves with various conditions (*i.e.*, healthy, poor and dwarf). However, the classification accuracies are higher than 80%, which could indicate that the classification based on proximal hyperspectral remote sensing techniques could be applied to separate mangrove forests of various health conditions. In addition, results from the one-way ANOVA indicate that there is a significant difference ($p < 0.05$) in the mean reflectance among the mangrove species and conditions (Table 5).

**Table 3.** Error matrix of the classification based on the seven selected wavebands.

| Type | DB | DR | PB | HR | HB | HW | Total | Users' Accuracy |
|---|---|---|---|---|---|---|---|---|
| DB | 30 | 0 | 0 | 0 | 0 | 0 | 30 | 100% |
| DR | 0 | 30 | 0 | 0 | 0 | 0 | 30 | 100% |
| PB | 2 | 0 | 28 | 0 | 0 | 0 | 30 | 93.33% |
| HR | 0 | 0 | 0 | 30 | 0 | 0 | 30 | 100% |
| HB | 1 | 0 | 1 | 0 | 29 | 0 | 31 | 93.55% |
| HW | 0 | 0 | 0 | 0 | 0 | 30 | 30 | 100% |
| Total | 33 | 30 | 29 | 30 | 29 | 30 | 181 | |
| Producer's accuracy | 90.91% | 100% | 96.55% | 100% | 100% | 100% | | |

Notes: HB, healthy black; DB, dwarf black; PB, poor condition black; HR, healthy red; DR, poor condition red; HW, healthy white.

**Table 4.** Error matrix of the classification validation based on the seven selected wavebands.

| Type | DB | DR | PB | HR | HB | HW | Total | Users' Accuracy |
|---|---|---|---|---|---|---|---|---|
| DB | 26 | 0 | 4 | 0 | 0 | 0 | 30 | 86.67% |
| DR | 0 | 29 | 0 | 1 | 0 | 0 | 30 | 96.67% |
| PB | 3 | 0 | 25 | 0 | 2 | 0 | 30 | 83.33% |
| HR | 0 | 0 | 0 | 30 | 0 | 0 | 30 | 100% |
| HB | 2 | 0 | 2 | 0 | 26 | 1 | 31 | 83.87% |
| HW | 0 | 0 | 0 | 0 | 0 | 30 | 30 | 100% |
| Total | 31 | 29 | 29 | 31 | 28 | 31 | 181 | |
| Producer's accuracy | 83.87% | 100% | 86.21% | 96.77% | 92.86% | 96.8% | | |

**Table 5.** Mean Square Between (MSB) and Mean Square within (MSW) variances of the mean reflectance at selected wavebands (mean squares).

| Waveband (nm) | 520 | 560 | 650 | 710 | 760 | 2100 | 2230 |
|---|---|---|---|---|---|---|---|
| MSB | 0.00274 | 0.00959 | 0.002211 | 0.035517 | 0.059308 | 0.010197 | 0.014219 |
| MSW | 0.00010 | 0.00022 | 0.000079 | 0.000651 | 0.000759 | 0.000148 | 0.000181 |

However, it is important to note that the extent of hyperspectral discrimination of mangroves from other mangrove zones located in both tropical and sub-tropical regions could vary depending on the influence of various factors, such as variable precipitation rates, soil salinity conditions and species composition. For semi-arid regions, as in this study, it is well known that the mangroves are under considerable stress due to soil hypersaline conditions and that such environmental factors induce seasonal changes in leaf pigments content, which, in turn, affect the hyperspectral reflectance of the selected mangrove species.

## 5. Conclusions

Mangrove forests represent one of the most important ecosystems in the world, and yet, they continue to experience considerable degradation. This study aimed to examine the separation of mangrove species with various health conditions using *in situ* hyperspectral data collected from mangrove leaves. The results of this study indicate that it is possible to select bands using a few statistical methods and then apply them, using a discriminant analysis based on quadratic discriminant functions, to classify mangroves with varying conditions. The results also indicate that spectrally, mangrove species and the conditions are distinct in various wavelength regions. Using various statistical techniques, the wavebands at 520, 560, 650, 710, 760, 2100 and 2230 nm were identified as the ideal bands for mangrove discrimination in this particular semi-arid region. Moreover, these bands are related to chlorophyll content, red edge, starch, cellulose, nitrogen and protein absorption. The classification and leave-one-out validation indicate that these wavebands are efficient for classifying mangroves with different health conditions. Generally, white and healthy red mangroves have the highest classification accuracy (100%) since they are spectrally distinct. It was also found that it is easiest to separate between healthy red and dwarf red mangroves due to the contrast in spectral properties. However, the greatest difficulty exists when attempting to separate black mangroves of various conditions (*i.e.*, healthy, dwarf, poor), especially between the poor and dwarf mangroves, due to the spectral similarity for the same species. Nonetheless, the classification accuracies were deemed satisfactory, even for the black mangrove classes. Moreover, the classification accuracies for validation were found to be generally higher than 80%. Consequently, the results of this investigation indicate that it is plausible to separate mangrove species with different health conditions using close-range hyperspectral data. Although detailed *in situ* hyperspectral assessments between mangroves is of utmost importance for accurate inter species discrimination, the aforementioned suggestions have to be considered when assessing spaceborne hyperspectral classification of mangrove areas.

## Acknowledgments

John M. Kovacs would like to acknowledge the financial support for the field work, which was provided through a discovery grant (#2014–06188) provided by the Natural Sciences and Engineering Research Council of Canada. Additional funding for the field campaigns was provided by Francisco Flores-Verdugo through the Instituto de Ciencias del Mar y Limnologia, UNAM, at Mazatlán station, Mexico. We would also like to thank the five anonymous reviewers who provided constructive comments and suggestions.

## Author Contributions

Chunhua Zhang and John M Kovacs designed the experiment. Chunhua Zhang, John M Kovacs, Francisco Flores-Verdugo and Francisco Flores-de-Santiago conducted the field work and laboratory data collection. Yali Liu, Chunhua Zhang, and John M Kovacs finished data analyses. Chunhua Zhang, John M Kovacs, Yali Liu, and Francisco Flores-Verdugo prepared the manuscript.

## Conflicts of Interest

The authors declare no conflict of interest.

## References


1. Krause, G.; Bock, M.; Weiers, S.; Braun, G. Mapping land cover and mangrove structures with remote sensing techniques: A contribution to a synoptic GIS in support of coastal management in North Brazil. *Environ. Manag.* **2004**, *34*, 429–440.
2. Kovacs, J.M.; Zhang, C.; Flores-Verdugo, F. Mapping coastal wetland using C-band ENVISAT ASAR and landsat optical data. *Cienc. Mar*. **2008**, *34*, 407–418.
3. Lee, T.; Yeh, H. Applying remote sensing techniques to monitor shifting wetland vegetation: A case study of Danshui River estuary mangrove communities, Taiwan. *Ecol. Eng*. **2009**, *35*, 487–496.
4. Gao, J. A comparative study on spatial and spectral resolutions of satellite data in mapping mangrove forests. *Int. J. Remote Sens*.**1999**, *20*, 2823–2833.
5. Green, E.P.; Clark, C.D.; Mumby, P.J.; Edwards, A.J.; Ellis, A.C. Remote sensing techniques for mangrove mapping. *Int. J. Remote Sens*.**1998**, *19*, 935–956.
6. Jensen, J. R.; Lin, H.; Yang, X.; Ramsey, E., III; Davis, B. A.; Thoemke, C.W. The measurement of mangrove characteristics in southwest Florida using SPOT multispectral data. *Geocarto. Int*. **1991**, *6*, 13–21.
7. Adam, E.; Mutanga, O.; Rugege, D. Multispectral and hyperspectral remote sensing for identification and mapping of wetland vegetation: A review. *Wetl. Ecol. Manag*. **2010**, *18*, 281–296.
8. Flores-de-Santiago, F.; Kovacs, J.M.; Flores-Verdugo, F. The influence of seasonality in estimating mangrove leaf chlorophyll-a content from hyperspectral data. *Wetl. Ecol. Manag*. **2013**, *21*, 193–207.
9. Zhang, C.; Liu, Y.; Kovacs, J.M.; Flores-Verdugo, F.; Flores-Santiago, F.; Chen, K. Spectral response to varying levels of leaf pigments collected from a degraded mangrove forest. *J. Appl. Remote Sens.* **2012**, *6*, 1–14.
10. Zhang, C.; Kovacs, J.M.; Wachowiak, M.P.; Flores-Verdugo, F. Relationship between hyperspectral measurements and mangrove leaf nitrogen concentrations. *Remote Sens*. **2013**, *5*, 891–908.
11. Hirano, A.; Madden, M.; Welch, R. Hyperspectral image data for mapping wetland vegetation. *Wetlands* **2003**, *23*, 436–448.
12. Green, E.P.; Mumby, P.J.; Edwards, A.J.; Clark, C.D.; Ellis, A.C. The assessment of mangrove areas using high resolution multispectral airborne imagery. *J. Coastal Res*. **1998**, *14*, 433–443.
13. Held, A.; Ticehurst, C.; Lymburner, L.; Williams, N. High resolution mapping of tropical mangrove ecosystems using hyperspectral and radar remote sensing. *Int. J. Remote Sens*. **2003**, *24*, 2739–2759.
14. Kamal, M.; Phinn, S. Hyperspectral data for mangrove species mapping: A comparison of pixel-based and object-based approach. *Remote Sens*. **2011**, *3*, 2222–2242.
15. Jensen, R.; Mausel, P.; Dias, N.; Gonser, R.; Yang, C.; Everitt, J.; Fletcher, R. Spectral analysis of coastal vegetation and land cover using AISA+ hyperspectral data. *Geocarto. Int*. **2007**, *22*, 17–28.
16. Demuro, M.; Chisholm, L. Assessment of Hyperion for Characterizing Mangrove Communities. Available online: http://url/?q=ftp://popo.jpl.nasa.gov/pub/docs/workshops/03_docs/Demuro_AVIRIS_2003_web.pdf (accessed on 19 August 2014).

17. Koedsin, W.; Vaiphasa, C. Discrimination of tropical mangroves at the species level with EO-1 hyperion data. *Remote Sens*. **2013**, *5*, 3562–3582.
18. Walters, B.B.; Ronnback, P.; Kovacs, J.M.; Crona, B.; Hussain, S.A.; Badola, R.; Primavera, J.H.; Barbier, E.; Dahdouh-Guebas, F. Ethnobiology, socio-economics and management of mangrove forests: A review. *Aquat. Bot*.**2008**, *89*, 220–236.
19. Hughes, G.F. On the mean accuracy of statistical pattern recognizers. *IEEE Trans. Inform. Theory* **1968**, *14*, 55–63.
20. Gomez-Chova, L.; Calpe, J.; Camps-Valls, G.; Martin, J.; Soria, E.; Vila, J.; Alonso-Chorda, L.; Moreno, J. Feature selection of hyperspectral data through local correlation and SFFS for crop classification. In Proceedings of IEEE International Geoscience and Remote Sensing Symposium, Toulouse, France, 21–25 July 2003; pp. 555–557.
21. Vaiphasa, C.; Skidmore, A.K.; de Boer, W.F.; Vaiphasa, T. A hyperspectral band selector for plant species discrimination. *ISPRS J. Photogramm*. *Remote Sens*. **2007**, *62*, 225–235.
22. Zhou, M.D.; Shu, J.O.; Chen, Z.G. Classification of hyperspectral remote sensing image based on genetic algorithm and SVM. *Proc. SPIE* **2010**, *7809*, doi:10.1117/12.860153
23. Zhuo, L.; Zheng, J.; Wang, F.; Li, X.; Ai, B.; Qian, J. A Genetic Algorithm Based Wrapper Feature Selection Method for Classification of Hyperspectral Images Using Support Vector Machine. Available online: http://en.cnki.com.cn/Article_en/CJFDTOTAL-DLYJ200803004.htm (accessed on 19 August 2014).
24. Sreekala, G.B.; Subodh, S.K. Hyperspectral data mining. In *Hyperspectral Remote Sensing of Vegetation*; Thenkabail, P.S., Lyon, G.J., Huete, A., Eds.; CRC Press: Boca Raton, FL, USA, 2011.
25. Schmidt, K.S.; Skidmore, A.K. Spectral discrimination of vegetation types in a coastal wetland. *Remote Sens. Environ*. **2003**, *85*, 92–108.
26. Thenkabail, P.S.; Enclona, E.A.; Ashton, M.S.; van Der Meer, B. Accuracy assessments of hyperspectral waveband performance for vegetation analysis applications. *Remote Sens. Environ*. **2004**, *91*, 354–376.
27. Vaiphasa, C.; Ongsomwang, S.; Vaiphasa, T.; Skidmore, A.K. Tropical mangrove species discrimination using hyperspectral data: A laboratory study. *Estuar. Coast. Shelf. Sci*. **2005**, *65*, 371–379.
28. Kamaruzaman, J.; Kasawani, I. Imaging spectrometry on mangrove species identification and mapping in Malaysia. *WSEAS Trans. Biol. Biomed*. **2007**, *8*, 118–126.
29. Mochel, J.; Ponzoni, F.J. Spectral Characterization of Mangrove Leaves in the Brazilian Amazonian Coast: Turiaçu Bay, Maranhão State. Available online: http://www.scielo.br/pdf/aabc/v79n4/a09v79n4.pdf (accessed on 19 August 2014).
30. Wang, L.; Sousa, W.P. Distinguishing mangrove species with laboratory measurements of hyperspectral leaf reflectance. *Int. J. Remote Sens*. **2009**, *30*, 1267–1281.
31. Flores-de-Santiago, F.; Kovacs, J.M.; Flores-Verdugo, F. Seasonal changes in leaf chlorophyll a content and morphology in a sub-tropical mangrove forest of the Mexican Pacific. *Mar. Ecol. Prog. Ser*. **2012**, *444*, 57–68.
32. Jain, N.; Ray, S.S.; Singh, J.P.; Panigrahy, S. Use of hyperspectral data to assess the effects of different nitrogen applications on a potato crop. *Precis. Agric*. **2007**, *8*, 225–239.

33. Cliff, N. The eigenvalues-greater-than-one rule and the reliability of components. *Psychol. Bull*. **1998**, *103*, 276–279.
34. Curran, P.J. Remote sensing of foliar chemistry. *Remote Sens. Environ.* **1989**, *30*, 271–278.
35. Salovaara, K.J.; Thessler, S.; Malik, R.N.; Tuomisto, H. Classification of Amazonian primary rain forest vegetation using Landsat ETM+ satellite imagery. *Remote Sens. Environ*. **2005**, *97*, 39–51.
36. Kovacs, J.M.; Liu, Y.; Zhang, C.; Flores-Verdugo, F.; de Santiago, F.F. A field based statistical approach for validating a remotely sensed mangrove forest classification scheme. *Wetl. Ecol. Manag.* **2011**, *19*, 409–421.
37. Lugo, A.E.; Ernesto M.; Cuevas, E.; Gilberto C.; Laboy Nieves, E.N.; Novelli, Y.S. Ecophysiology of a mangrove forest in Jobos Bay, Puerto Rico. *Caribb. J. Sci.* **2007**, *43*, 200–219.
38. Lovelock, C.E.; Bali, M.C.; Choat, B.; Engelbrecht, B.M.J.; Holbrook, N.M.; Feller, I.C. Linking physiological processes with mangrove forest structure: Phosphorus deficiency limits canopy development, hydraulic conductivity and photosynthetic carbon gain in dwarf Rhizophora mangle. *Plant Cell. Environ*. **2006**, *29*, 793–802.
39. Feller, I.C. Effects of nutrient enrichment on growth and herbivory of dwarf red mangrove (Rhizophora mangle). *Ecol. Monogr*. **1995**, *65*, 477–505.
40. Flores-de-Santiago, F.; Kovacs, J.M.; Flores-Verdugo, F. Assessing the utility of a portable pocket instrument for estimating seasonal mangrove leaf chlorophyll contents. *Bull. Mar. Sci*. **2013**, *89*, 621–633.
41. Blackmer, T.M.; Schepers, J.S.; Varvel, G.E.; Walter-Shea, E.A. Nitrogen deficiency detection using reflected shortwave radiation from irrigated corn canopies. *Agron. J*. **1996**, *88*, 1–5.
42. Carter, G.A.; Miller, R.L. Early detection of plant stress by digital imaging within narrow stress-sensitive wavebands. *Remote Sens. Environ*. **1994**, *50*, 295–302.
43. Carter, G.A.; Knapp, A.K. Leaf optical properties in higher plants: Linking spectral characteristics to stress and chlorophyll concentration. *Am. J. Bot*. **2001**, *88*, 677–684.